Cnossen, I., Matzka, J. (2016): Changes in solar quiet magnetic variations since the Maunder Minimum: A comparison of historical observations and model simulations. - *Journal of Geophysical Research*, *121*, 10, pp. 10,520—10,535.

DOI: http://doi.org/10.1002/2016JA023211

AGU PUBLICATIONS

JGR

Journal of Geophysical Research: Space Physics

RESEARCH ARTICLE
10.1002/2016JA023211

**Key Points:**
- Historic observations of daily magnetic variations in 1782-1783 and 1841-1842 show notable differences with modern data from 2010
- Changes in the position of the magnetic equator and main magnetic field intensity can explain some of these differences
- Long-term changes in solar activity have effects of comparable magnitude only in regions where main field changes have been small

**Supporting Information:**
- Supporting Information S1
- Movie S1
- Movie S2
- Movie S3
- Movie S4
- Movie S5
- Movie S6

**Correspondence to:**
I. Cnossen,
icnossen@yahoo.com

**Citation:**
Cnossen, I., and J. Matzka (2016), Changes in solar quiet magnetic variations since the Maunder Minimum: A comparison of historical observations and model simulations, *J. Geophys. Res. Space Physics*, *121*, 10,520–10,535, doi:10.1002/2016JA023211.

Received 20 JUL 2016
Accepted 27 SEP 2016
Accepted article online 29 SEP 2016
Published online 26 OCT 2016



# Changes in solar quiet magnetic variations since the Maunder Minimum: A comparison of historical observations and model simulations

**Ingrid Cnossen[1] and Jürgen Matzka[1]**

[1]GFZ German Research Centre for Geosciences, Potsdam, Germany

**Abstract** Magnetic measurements going back to the eighteenth century offer a unique opportunity to study multicentennial changes in the upper atmosphere. We analyzed measurements from Rome and Mannheim from May 1782 to May 1783 and measurements from Greenwich, St. Helena, Cape of Good Hope, and Singapore from May 1841 to May 1842. A comparison of the daily magnetic variations in these historical data with modern-day observations from 2010 at nearby stations (where available) showed notable differences in the amplitude and/or phase of the *X* and *Y* components. Model simulations indicated that these can be explained at least to some extent by changes in the Earth's main magnetic field. Changes in the main field strength and the northwestward movement of the magnetic equator, in particular in the region of the South Atlantic Anomaly, have caused changes in the positioning, shape, and strength of the equivalent current vortices in the ionosphere that result in the magnetic perturbations on the ground. Differences in solar activity between the historical and modern epochs, which were all near solar minima, were too small to have a notable effect on the ground magnetic perturbations. However, in regions where main magnetic field changes have been relatively small for the last ~400 years, e.g., in Singapore, the effects of a long-term increase in solar activity from Maunder Minimum conditions to normal solar minimum conditions (an increase in $F_{10.7}$ of ~35 solar flux units) were comparable to the effects of geomagnetic main field changes.

## 1. Introduction

Solar quiet (*Sq*) magnetic variations arise from daytime currents in the low-latitude to midlatitude ionosphere, driven by upper atmospheric winds. The winds are generated by the daily variation in the absorption of solar radiation and move the ionospheric plasma through the Earth's magnetic field. This creates an upper atmosphere dynamo, which produces a regular current pattern when geomagnetic activity is low that manifests itself as regular magnetic variations on the ground. The dayside equivalent *Sq* current system, i.e., the horizontal currents overhead that would produce the observed dayside magnetic perturbations on the ground, consists of a clockwise current vortex in the Southern Hemisphere and counterclockwise current vortex in the Northern Hemisphere.

The *Sq* current system is sensitive to the solar activity level, primarily because higher solar radiative emissions increase the conductivity of the ionosphere [e.g., *Rastogi and Iyer*, 1976; *Yamazaki et al*., 2011; *Takeda*, 2013]. During the Maunder Minimum, a period of extremely low solar activity from ~1645 to ~1715, we would therefore expect to observe much weaker daily *Sq* variations. Any variations in solar activity that have occurred since then [e.g., *Krivova et al*., 2010] also have the potential to cause variations in ground magnetic perturbations. The *Sq* variation is mainly sensitive to solar radiation in the extreme ultraviolet (EUV), which is characterized quite well by the $F_{10.7}$ index [e.g., *Briggs*, 1984; *Yamazaki et al*., 2010]. Figure 1 shows how $F_{10.7}$ has changed since the Maunder Minimum, based on the reconstruction of solar spectral irradiance by *Krivova et al*. [2010] (see section 2 for further details).

A second important factor that influences the *Sq* current system is the secular variation of the Earth's main magnetic field [e.g., *Takeda*, 2013; *Cnossen and Richmond*, 2013]. The ionospheric conductivity is inversely related to the main field strength [e.g., *Richmond*, 1995; *Cnossen et al*., 2011], while the orientation of the magnetic field influences the effectiveness of the neutral wind dynamo [e.g., *Cnossen and Richmond*, 2008, 2012]. Further, the geographic positioning of important features of the main field, such as the magnetic equator, affects the magnetic perturbations that are observed at a fixed location on the ground, e.g., at a magnetic

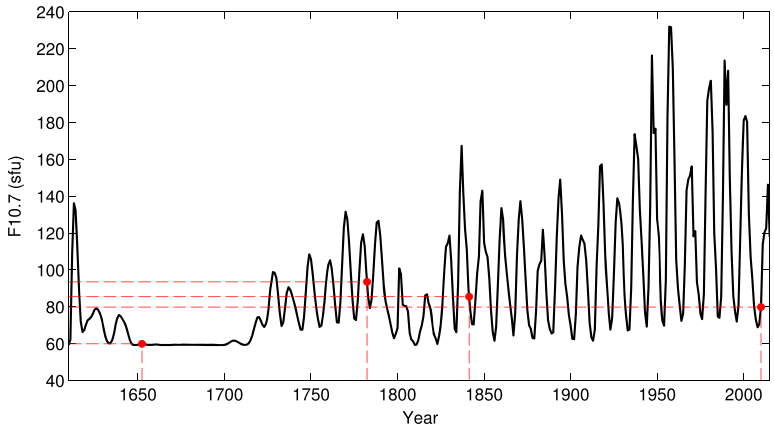


**Figure 1.** Reconstruction of *F*10.7 since 1610 based on the reconstruction of solar spectral irradiance by *Krivova et al*. [2010]. Red dots mark years relevant for our study.

observatory. The Earth's magnetic field has changed considerably since the 1600s, as illustrated in Figure 2. In most places the magnetic field strength has decreased, and this is especially prominent in the South Atlantic Anomaly (SAA) region, also known as the South Atlantic Magnetic Anomaly (SAMA), where the magnetic field is already unusually weak. This region of weak magnetic field has expanded over time and also moved westward. Other features of the magnetic field, such as the magnetic equator and the magnetic dip poles, also show a westward movement, as well as a northward shift, in particular in the SAA region. These main magnetic field changes are another potential source of long-term variations in magnetic perturbations observed at the ground.

Previous studies have examined trends in *Sq* magnetic variations for (portions of) the past century [*Sellek*, 1980; *Schlapp et al*., 1990; *Macmillan and Droujinina*, 2007; *Torta et al*., 2009; *Elias et al*., 2010; *De Haro Barbas et al*., 2013; *Takeda*, 2013; *Shinbori et al*., 2014; *Yamazaki and Kosch*, 2014]. These studies confirmed that both the Sun and the Earth's magnetic field affect multidecadal variations in the *Sq* system, though their relative importance depends on the location and on the time interval studied. In addition, it has been suggested that the steady increase in atmospheric greenhouse gas concentrations could affect *Sq* magnetic perturbations observed on the ground, due to changes in the electron density distribution associated with upper atmospheric cooling and contraction [*Rishbeth and Roble*, 1992; *Elias et al*., 2010] and/or due to changes in upwardly propagating tidal waves from the lower atmosphere [*Yamazaki and Kosch*, 2014]. However, model simulations by *Cnossen* [2014] indicated that at least the former effects of increased greenhouse gas concentrations on *Sq* variations are negligibly small.

*Sq* magnetic variations are one of the few observables indicative of upper atmosphere processes and long-term trends that go back to the eighteenth century. In this study we will examine how *Sq* magnetic variations have changed since the Maunder Minimum period, based on model simulations combined with historical magnetic observations made in the eighteenth and nineteenth centuries. The model simulations will also be used to disentangle the role of solar activity and main magnetic field variations in causing observed differences in magnetic perturbations for different historical periods. The rest of this paper is organized as follows. Section 2 describes the historical data from the eighteenth and nineteenth centuries analyzed here, as well as the modern data used for comparison. Section 3 describes the model simulations that we compare with. Results are presented in section 4, followed by a summary and conclusions in section 5.

## 2. Observations

We analyze data from the 1840s from four geomagnetic observatories: Greenwich (GRW), Cape of Good Hope (CGH), St. Helena (SHE), and Singapore (SIN). These are among the stations established under Edward Sabine in the British Empire, in close cooperation with the Göttingen Magnetic Union (for an account of historical and modern geomagnetic observatories, see, e.g., *Matzka et al*. [2010]). Both spot readings of the geomagnetic field (together with ambient temperature) and derived data products can be found in the yearbooks

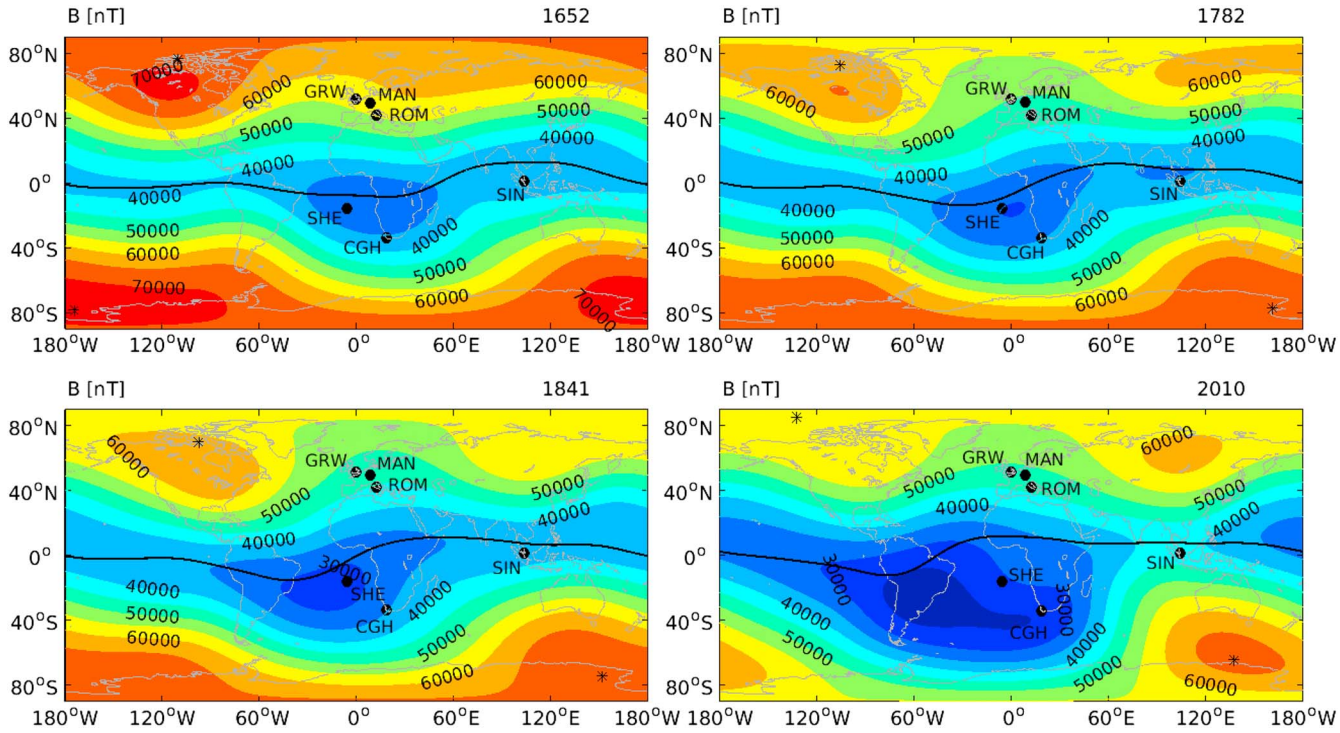


**Figure 2.** Main magnetic field intensity (color contours) in (top left) 1652, (top right) 1782, (bottom left) 1841, and (bottom right) 2010. Also marked are the positions of the magnetic equator (solid line) and magnetic dip poles (stars) according to the GUFM1 model (for 1652, 1782, and 1841) and the IGRF (for 2010). The locations of magnetic stations for which we analyze historical data (see section 2 and Table 1) are indicated with black dots.

detailing these observations from the 1840s onward. Spot readings were typically obtained every hour or every even hour Göttingen time from Mondays to Saturdays. Time stamps in the yearbooks are 00 h at noon and 12 h at midnight (i.e., astronomical reckoning) and are given either in Göttingen mean time or the corresponding local mean time.

The data used for our study were read from digital scans of the yearbooks provided by the British Geological Survey (BGS) and manually typed into files. GRW data were taken from Tables VI, XIX, and XXXI in *Airy* [1843] and Tables XI, XXVII, and XLI in *Airy* [1846]; CGH data were taken from pp. 2–19 and Tables XI and XVI in *Sabine* [1851]; SHE data were taken from Tables IV, XI, and XIV in *Sabine* [1847]; and SIN data were taken from Tables I, III, and V in *Elliot* [1851]. We used tables that give the mean daily variation for each month, such that each value is deduced from all observations taken at that hour in the respective month (e.g., the mean of all observations taken at 10 h Göttingen mean time in August 1841). Unlike the spot readings listed in the yearbooks, the monthly mean data values are already corrected for the effects of ambient temperature on the classical magnetometers, which is an advantage. On the other hand, by taking the monthly mean values, we cannot select data from geomagnetically quiet days only. For all four stations we selected the data available between May 1841 and May 1842 inclusive for our study.

Horizontal and vertical magnetic field strength in the tables are given in parts per million of the total $H$ and $Z$ components. In order to convert to nanotesla, we used appropriate absolute values taken from the annual observatory means catalogue of the World Data Centre (WDC) of Geomagnetism, Edinburgh, or model predictions from GUFM1 [*Jackson et al.*, 2000]. The magnetic declination for SHE and SIN is given as a deviation from a baseline, and we transferred these into approximate absolute values again using either the observatory annual means from the WDC or GUFM1. The sign of the declination was changed according to modern convention from westerly to easterly. The $H$ and $Z$ components were not available for all months. If the $H$ component was available, we transformed $H$ and $D$ to $X$ and $Y$ for further analysis. For the $Sq$ variations, the $Z$ component typically has the smallest amplitude and is more strongly affected by induction effects such as the ocean effect [*Kuvshinov et al.*, 2007; *Kuvshinov*, 2008]. Therefore, we do not analyze the $Z$ component here.

**Table 1.** Overview of Locations and Data Availability for Historical Stations and Locations of Nearby Modern Stations

| Historical Station | Abbreviation | Geographic Location | Time Period | Components | Modern Station | Abbreviation | Geographic Location |
|---|---|---|---|---|---|---|---|
| Rome | ROM | 41.8°N/12.5°E | May 1782 to Apr 1783 | *D* | l'Aquila | AQU | 42.4°N/13.3°E |
| Mannheim | MAN | 49.5°N/8.5°E | May 1782 to Apr 1783 | *D* | Black Forest | BFO | 48.3°N/8.3°E |
| Greenwich | GRW | 51.5°N/0°E | May 1841 to May 1842 | *D*, *H*, *X*, *Y* | Hartland | HAD | 51.1°N/4.5°W |
| Cape of Good Hope | CGH | 33.9°S/18.5°E | May 1841 to May 1842 | *D*; from Oct 1841: *H*, *X*, *Y* | Hermanus | HER | 34.4°S/19.2°E |
| St. Helena | SHE | 15.9°S/5.7°W | May 1841 to May 1842 | *D*, *H*, *X*, *Y* | St. Helena | SHE | 16.0°S/5.8°W |
| Singapore | SIN | 1.3°N/103.9°E | May 1841 to May 1842 | *D*, *H*, *X*, *Y* | N/A | N/A | N/A |

In the early 1780s a network of meteorological and magnetic stations, most of them in Europe, was set up by the Societas Palatina [*Hemmer*, 1783]. Readings of declination were performed with a compass needle three times per day with the help of a vernier and an angular resolution of 3 arc min was achieved. Annual means derived from these measurements were previously reported and studied by, e.g., *Hansteen* [1819] and *Korte et al*. [2009], but here we analyze the spot readings of the declination (*D*) from May 1782 to May 1783 for the two stations Rome (ROM) and Mannheim (MAN), which we took from the Societas Palatina yearbooks for the respective years [*Hemmer*, 1784, 1785]. At Rome, observations were made by Guiseppe Calandrelli in the Collegio Romano [*Hemmer*, 1783, p. 306], while Johann Jakob Hemmer was in charge of the observations in Mannheim. The timing of the measurements is 7 A.M., 2 P.M., and 9 P.M.. In the literature on the meteorological data from these stations, the time system for these time stamps is given as mean solar time [*Camuffo*, 2002 (p. 342); *Winkler*, 2009]. Accurate knowledge of the timing of historical temperature readings is important for climate studies, and therefore, this subject is well investigated [*Camuffo*, 2002]. For our analysis, we therefore also assume the time stamps to be mean solar time. Nevertheless, there could in principle be two sources of error here: if Mannheim mean time instead of Rome mean time was used in Rome, this would add an error of 16 min (Rome is 4° farther east than Mannheim), and hence, we would have to add to our UTC time stamp 16 min. Using apparent solar time instead of mean solar time would add an error of ±16.5 min, depending on the season. At Rome, the daily pattern of the *D* readings is quite regular, as expected for *Sq*. For time stamps with declination data deviating from this regular pattern, the more northerly stations at Mannheim and Copenhagen (not shown here) often show larger amplitude deviations, which we interpret as deviations from *Sq* due to ionospheric currents during geomagnetic storms. This gives confidence in the quality of the data. To reconstruct the daily variation for each month and diminish the influence of geomagnetic storms and other irregular variations in this data set, we calculated median values over all days of the month for 7 A.M., 2 P.M., and 9 P.M., respectively.

We compare the historical data with modern-day data taken from nearby stations where possible, as indicated in Table 1. For this we selected data from the full year 2010 (January–December), taken from the Intermagnet website (www.intermagnet.org), because a model simulation for this year was already available as well. Only modern SHE data were taken directly from our own records, as this station is managed

**Table 2.** Overview of TIE-GCM Simulations[a]

| Identifier | Magnetic Field | $F_{10.7}$ Index | *Kp* Index |
|---|---|---|---|
| yr165253 F60 | 1652–1653 (GUFM1) | 60 (SATIRE) | 1 |
| yr165253 F95 | 1652–1653 (GUFM1) | 95 | 1 |
| yr178283 | 1782–1783 (GUFM1) | 95 (SATIRE) | 1 |
| yr184142 | 1841–1842 (GUFM1) | 85 (SATIRE) | 1 |
| yr184142 F95 | 1841–1842 (GUFM1) | 95 | 1 |
| yr2010 | 2010 (IGRF-11) | As observed (~80) | As observed (~1+) |

[a]For the magnetic field and the $F_{10.7}$ index the model used (if any) is indicated in brackets.

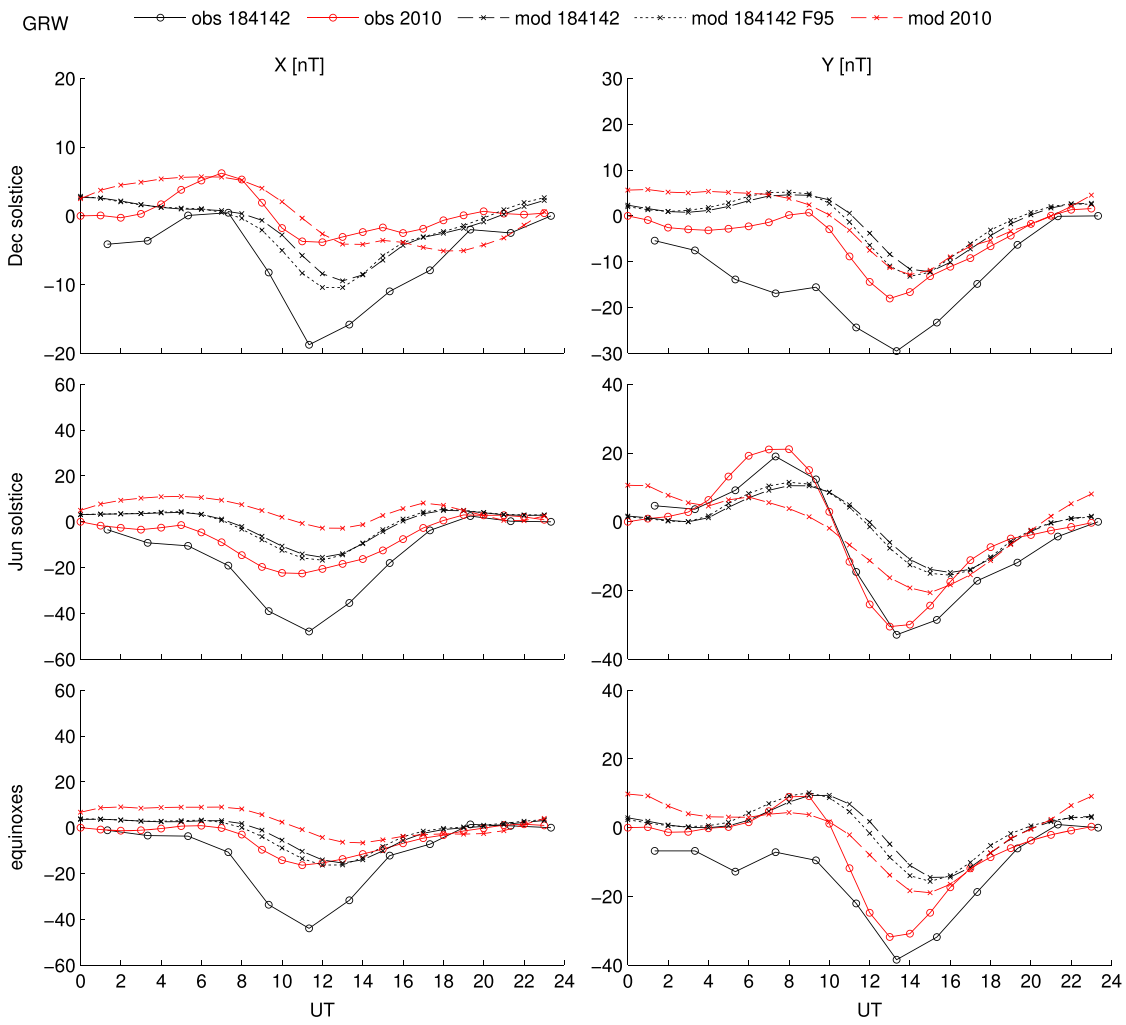


**Figure 3.** (a) Daily magnetic variations in the *X* (left column) and *Y* (right column) components at GRW around December solstice (top), June solstice (middle), and the equinoxes (bottom) as observed (solid lines/open circles) and simulated (dashed lines/crosses) in 1841–1842 (black) and 2010 (red). The simulation with $F_{10.7}$ set to 85 sfu is indicated with long dashes and the one with $F_{10.7}$ set to 95 sfu with short dashes. (b) Same as Figure 3a but for SHE and showing only the 1841–1842 simulation with $F_{10.7}$ set to 85 sfu. (c) Same as Figure 3b but for CGH. (d) Same as Figure 3b but for SIN. Note that modern-day observations for 2010 are missing in this case.

by Deutsches GeoForschungsZentrum (GFZ). This time series is also available as a separately published data set [*Matzka*, 2016]. Monthly mean values for each UT were calculated from the minute data. For both the historical and modern data we subtracted the local midnight value to obtain the daily variation, which we interpret as *Sq*. Since it was not possible to select only quiet days for the observations in the 1840s, which would be the preferred method of estimating *Sq*, both the historical and the modern mean daily variations we analyze here are based on means over all days, regardless of magnetic disturbance level. This approach is justified, as we are close to solar minimum and a comparison of means from quiet days only (defined here as days for which $Kp \leq 2$) with means from all days showed very similar results for the modern data (not shown).

To analyze the daily variations, we group the data into four seasons: June solstice (May, June, July, and August), December solstice (November, December, January, and February), and the equinoxes (March, April, September, and October). Preliminary analysis showed that the daily variation averaged over these months gives a reasonable representation of the daily variation in each individual month for both the historical and modern data, as well as the simulation results. Note that in case of the historical data, not all months are always available, while the month of May may be available twice (see Table 1). In all cases we use all available data to calculate seasonal averages.

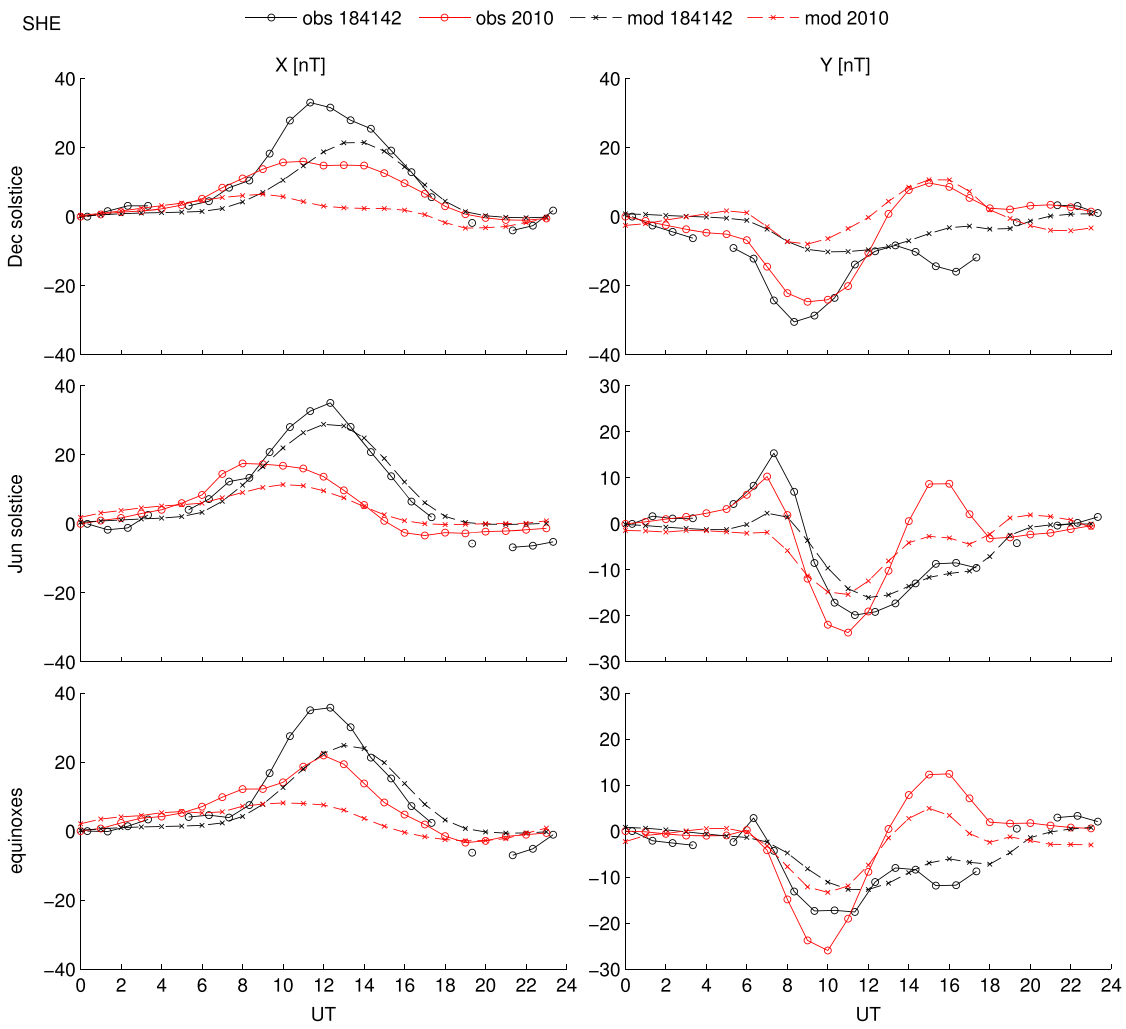


**Figure 3.** (continued)

## 3. Model and Simulation Setup

We use the Thermosphere-Ionosphere-Electrodynamics General Circulation Model (TIE-GCM [*Roble et al*., 1988; *Richmond et al*., 1992]) to determine the extent to which differences between observed magnetic perturbations for different periods can be attributed to the Sun and the Earth's magnetic field as well as to study the *Sq* system during the Maunder Minimum period. The TIE-GCM is a time-dependent, three-dimensional model that solves the fully coupled, nonlinear, hydrodynamic, thermodynamic, and continuity equations of the thermospheric neutral gas self-consistently with the ion continuity equations. In the setup used here, the model grid consists of 72 latitude and 144 longitude points (2.5° × 2.5° resolution) and 57 pressure levels between ~96 and ~500 km.

The TIE-GCM has previously been used to study how changes in the geomagnetic field since 1900 have affected the thermosphere-ionosphere system [*Cnossen and Richmond*, 2008, 2013; *Cnossen*, 2014]. These studies used the International Geomagnetic Reference Field (IGRF) [*Thébault et al*., 2015] to define the main magnetic field, which only goes back to 1900. To go back further in time, we therefore have to rely on a different magnetic field model. Here we used the GUFM1 model by *Jackson et al*. [2000], which assumes a decay in $g_1^0$ of 15 nT/year prior to 1840, while from 1840 onward the field intensity is determined by observations.

Model experiments were performed for 13 month intervals from May 1841 to May 1842 and from May 1782 to May 1783 for comparison with the observed daily magnetic variations described in section 2.

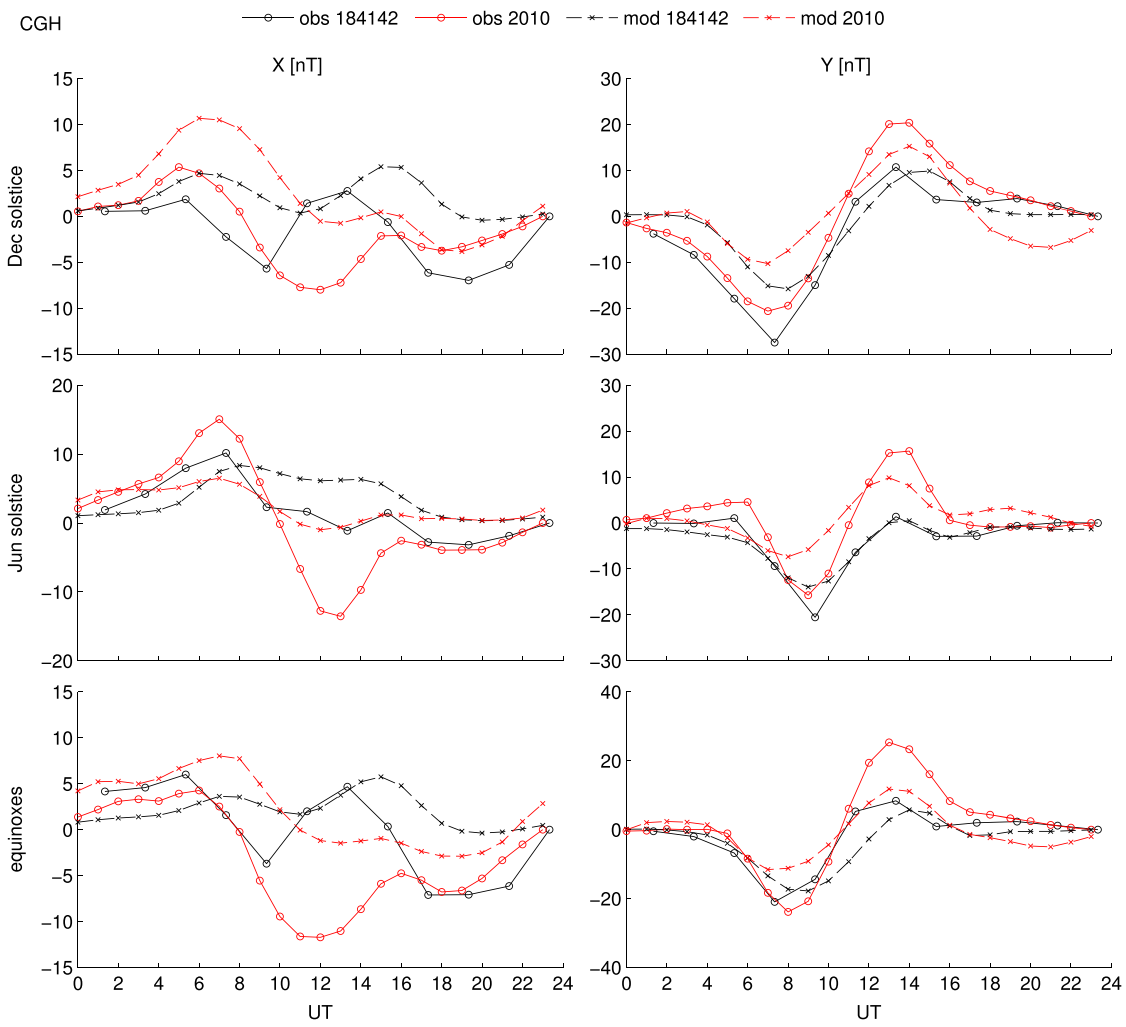


**Figure 3.** (continued)

Two further historical simulations were conducted for a similar interval within the Maunder Minimum, from May 1652 to May 1653. A present-day simulation for the full year 2010 was done for comparison with the historical simulations.

Solar and geomagnetic activity levels were specified through the $F_{10.7}$ radio flux and *Kp* indices, respectively. Observations of $F_{10.7}$ only go back to 1947. We therefore used a reconstruction of $F_{10.7}$ going back to 1610 (N. Krivova, personal communication, 2016) to specify solar activity levels for earlier time periods. This reconstruction was done with the Spectral And Total Irradiance Reconstruction (SATIRE) model [*Krivova et al.*, 2010]. Based on the reconstruction, a constant $F_{10.7}$ value was set throughout the simulation interval for each historical simulation (see Table 2), since the reconstruction does not have sufficient temporal resolution (1 year) to justify time-varying inputs. For the 1652–1653 and 1841–1842 intervals additional simulations were done to match the $F_{10.7}$ index of 95 solar flux units (sfu) of the 1782–1783 interval to control for the effects of differences in solar activity levels between different historical periods. The geomagnetic *Kp* index for all the historical simulations was set to a constant low value of 1, as we are interested in quiet conditions and there is no observational information available that could be used to set more realistic values. However, the present-day simulation used time-varying, observed $F_{10.7}$ and *Kp* values as input, as this should give a better comparison with modern observations. On average, the $F_{10.7}$ index for 2010 was ~80 solar flux units (sfu) and the *Kp* index ~1+.

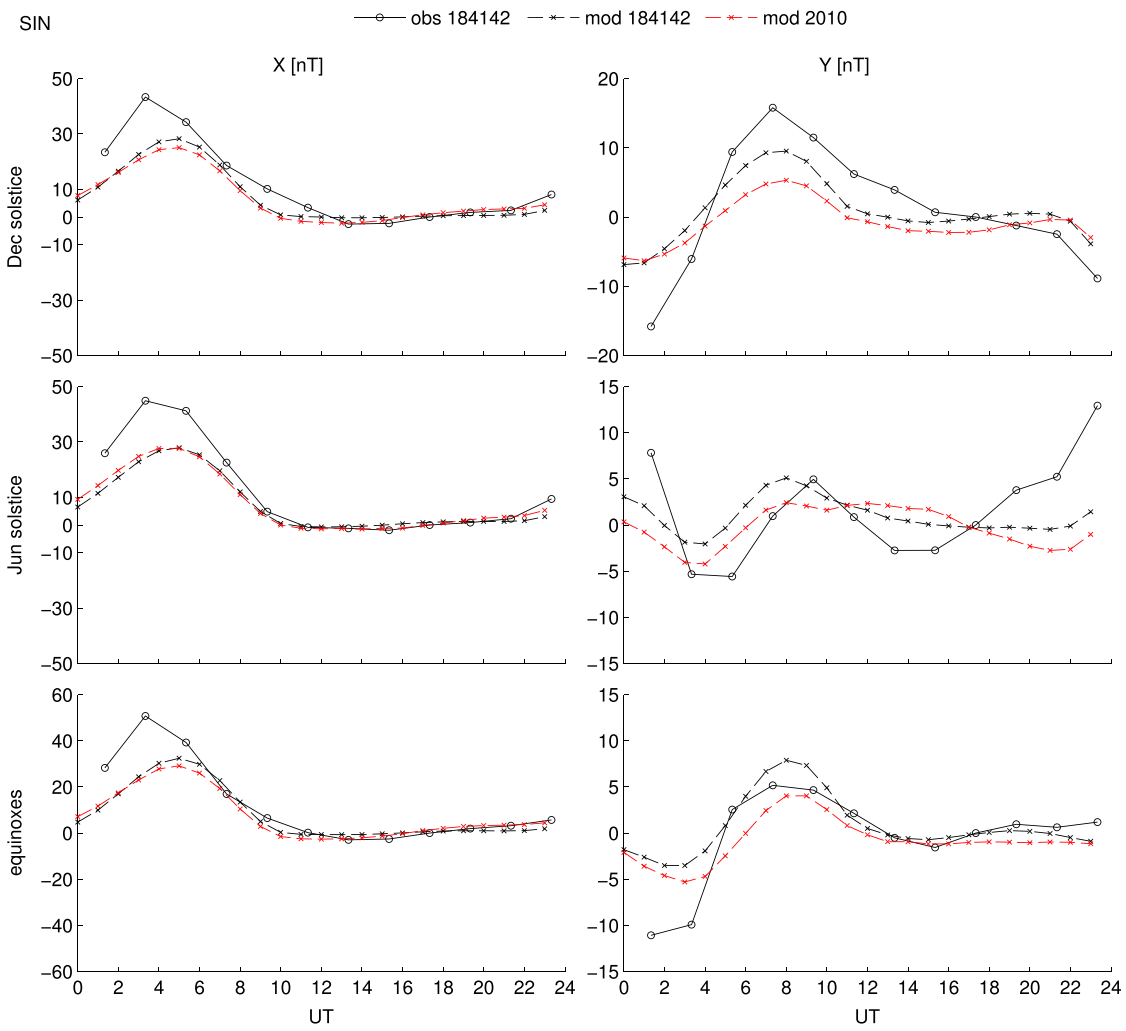


**Figure 3.** (continued)

Magnetic perturbations on the ground were calculated with a postprocessing code described by *Doumbia et al.* [2007] and *Richmond and Maute* [2014]. This includes only perturbations associated with currents flowing in the ionosphere and geomagnetic field-aligned currents above the ionosphere. Currents induced in the Earth by these time-varying external currents are taken into account by assuming a perfectly conducting layer at a depth of 600 km. Any effects of currents flowing perpendicular to the geomagnetic field in the magnetosphere are not considered, apart from fictitious radial currents flowing to or from infinity at each field line apex, needed to balance any net field-aligned current flowing into or out of the ionosphere on a field line. However, given that we are studying just the *Sq* current system, which is associated with the low-latitude to midlatitude ionospheric wind dynamo, this limitation is not important here. We do note that the TIE-GCM tends to underestimate *E* region electron densities and conductivities and therefore also tends to underestimate magnetic perturbations.

## 4. Results

### 4.1. *X* Variations at GRW, SHE, CGH, and SIN: 1841–1842 Versus 2010

Figures 3a–3d show the daily magnetic variation in the *X* and *Y* components at GRW, SHE, CGH, and SIN for each of the three seasons as observed and modeled in 1841–1842 and 2010. Since the *Sq* current system is a daytime phenomenon, we will concentrate on the daytime magnetic variations. We first discuss variations in

the *X* component, which are associated with east-west directed currents, while variations in the *Y* component for the same stations will be studied in section 4.2.

The main feature of the daytime magnetic variation in the *X* component at GRW is the depression around 8–16 UT which is associated with the westward current poleward of the *Sq* current focus, which sweeps past the station over the course of a day. The observations show that this depression is larger in 1841–1842 than in 2010 for all seasons, though this is clearest around June solstice (i.e., in summer). The model results also show a larger depression around noon for 1841–1842 than for 2010, but the simulated magnetic variations are generally more positive than observed. This could be due to the underestimation of *E* region conductivities, and hence of the *Sq* magnetic variations, by the TIE-GCM. The two simulations for 1841–1842, with slightly different solar activity levels, show very similar magnetic variations, indicating that the observed differences between the magnetic variations in 1841–1842 and 2010 are unlikely to be caused by different solar activity levels. This is also the case for the other stations we analyze here. In Figures 3b–3d we therefore only show results for the 1841–1842 simulation with $F_{10.7}$ set to 85 sfu. There are notable differences between the 1841–1842 simulations and the one for 2010, which suggest that differences in the Earth's main magnetic field do play a role in causing the observed differences between the magnetic variations in 1841–1842 and 2010.

We examine how the Earth's main magnetic field affects the daily variation at GRW by studying the simulated equivalent current functions for 1841–1842 and 2010. The equivalent current function $\Psi$ is related to the equivalent current density, $\mathbf{K}_{eq}$, as [e.g., *Murison et al.*, 1985]

$$\mathbf{K}_{eq} = -\hat{z}\times\nabla\psi \tag{1}$$

Where $\hat{z}$ is a unit vector in the downward direction. The horizontal gradient of the equivalent current function describes the fictitious horizontal current system that would produce the same magnetic perturbations on the ground as the actual three-dimensional current system that the model solves for. This fictitious equivalent current flows along isocontours of the equivalent current function, anticlockwise around minima and clockwise around maxima. This way the two main *Sq* current vortices, as well as their changes in shape and position with a changing geomagnetic main field, can be easily visualized.

Figure 4 shows an example of the equivalent current function for the 2010 and 1841–1842 simulations at 12 UT for June solstice. The locations of the *Sq* current foci (the maximum and minimum of the equivalent current function) are marked with white stars. Note that a station located poleward of the *Sq* focus in either hemisphere experiences a westward current around noon, and therefore a negative magnetic perturbation in the *X* component, while a station equatorward of the *Sq* focus experiences an eastward current, and therefore a positive magnetic perturbation around noon in the *X* component. Movies showing the temporal evolution of the equivalent current function during one full day for each season and epoch can be found in the supporting information.

The shape and strength of the current vortices have changed considerably between 1841–1842 and 2010. The current vortex in the Northern Hemisphere has become weaker, while the vortex in the Southern Hemisphere has become stronger. This strengthening of the Southern Hemisphere vortex is likely to be related to the weakening of the main field there (see Figure 2), which results in increased ionospheric conductivity [e.g., *Cnossen et al.*, 2011, 2012]. The weakening of the vortex in the Northern Hemisphere is more likely caused by the northwestward movement of the *Sq* focus, which places it in the morning sector at higher geographic latitude rather than around noon nearer the equator, resulting in reduced ionospheric conductivity due to decreased EUV ionization. The northwestward movement of the Northern Hemisphere *Sq* focus mimics the northwestward movement of the magnetic equator in this region (see Figure 2).

The changes in the positioning and strength of the Northern Hemisphere current vortex can explain the changes in the daily magnetic variation at GRW. In 1841–1842, GRW was located on the poleward edge of the Northern Hemisphere *Sq* vortex, in a location with strong westward currents. However, in 2010 GRW was located only slightly farther north than the *Sq* focus, i.e., in a location where there are no strong east-west currents. Together with the weakening of the Northern Hemisphere current vortex as a whole, this has caused the daily variation in the *X* component at GRW to be much weaker in 2010 than in 1841–1842. Based on Figure 3a, it appears that the model simulations still underestimate this effect somewhat, as the simulated difference between 1841–1842 and 2010 is smaller than the observed difference between these epochs.

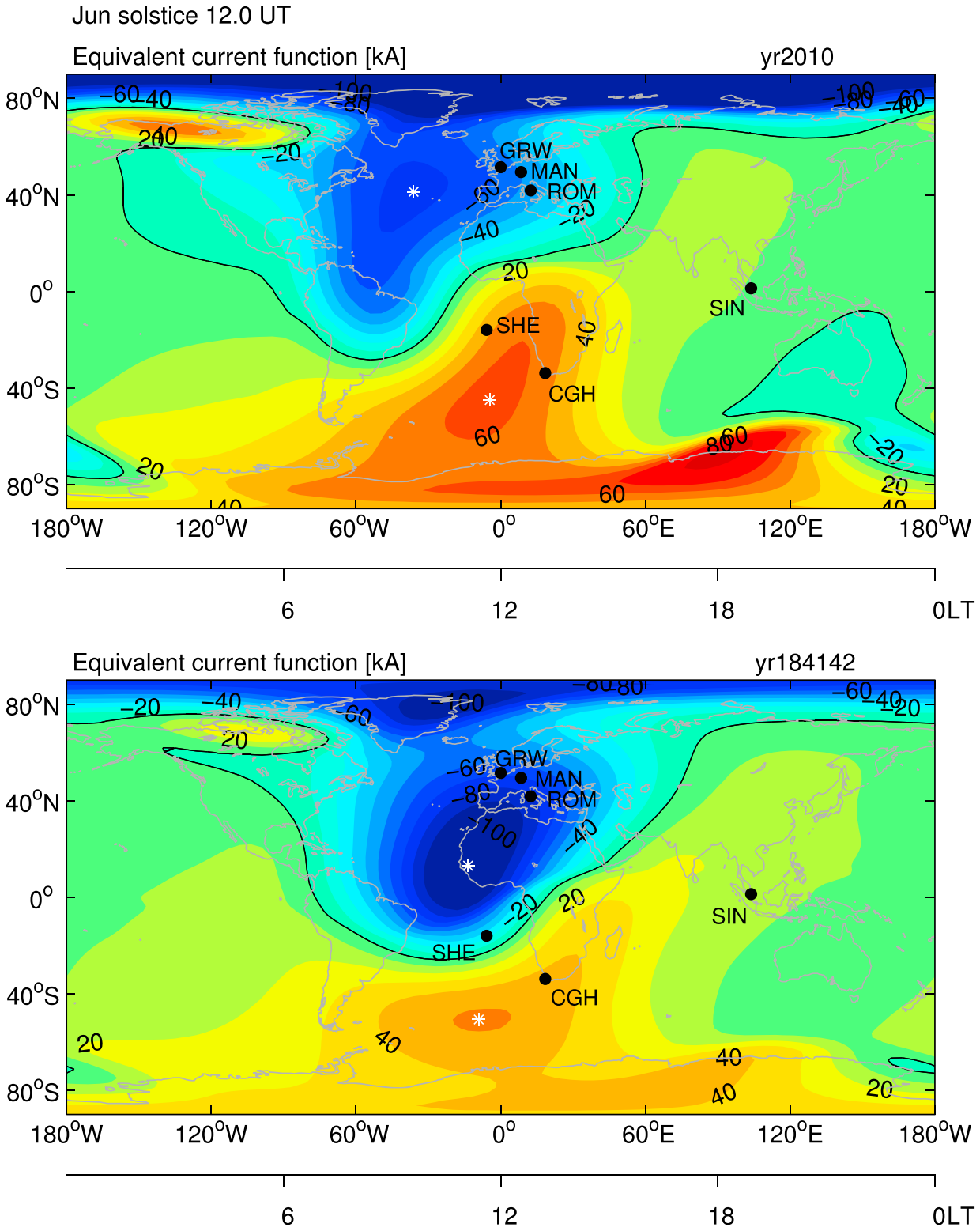


**Figure 4.** Simulated equivalent current function in 2010 (top) and 1841-42 (bottom) at 12 UT for June solstice. Station locations are marked with black dots and the positions of the Sq foci with white stars.

This may be so because the TIE-GCM does not reproduce the *Sq* current system perfectly, although we cannot rule out that some process other than the secular variation of the main magnetic field could also have contributed to the observed differences between 1841–1842 and 2010.

The observed magnetic variations in the *X* component at SHE, shown in Figure 3b, show very clearly a peak around 12 UT which is much stronger in 1841–1842 than in 2010, and this is quite well reproduced by the model simulations. Figure 4 shows that SHE was located very close to the zero line of the equivalent current function between the Northern and Southern Hemisphere current vortices in 1841–1842 and therefore experienced a strong eastward current during the day, resulting in a strong northward magnetic perturbation. In 2010, the station was located farther away from the zero line, closer to the *Sq* focus in the Southern Hemisphere. In principle this on its own should lead to weaker eastward currents. However, the shape of the Southern Hemisphere vortex has also changed considerably, in such a way that the eastward current at SHE is reduced for 2010 compared to 1841–1842 (the contours of the equivalent current function become more north-south than east-west oriented). Both factors thereby contribute to a weaker northward magnetic perturbation in 2010.

The variations in the *X* component at CGH (Figure 3c) are much more complicated than at GRW and SHE and generally quite weak. This is because CGH is located quite close to the *Sq* focus of the Southern Hemisphere in terms of latitude, so that it tends to experience only weak east-west directed currents. Further, CGH is located in a region where the shape of the current vortex departs considerably from a circular shape due to the nondipolar structure of the main magnetic field in this region. This means that the daily variation in the *X* component at CGH does not follow a standard pattern.

The observations indicate notable differences between 1841–1842 and 2010, which is understandable given that CGH is located in a region where main magnetic field changes have been relatively large. However, the daily variation in the *X* component and the differences between 1841–1842 and 2010 are generally not very well reproduced by the model simulations, although some features do correspond. For instance, for June solstice around 12 UT, both the observations and simulations show a relatively more positive magnetic perturbation for 1841–1842 than for 2010. Based on Figure 4, we can infer that this is probably due to the change in the shape of the Southern Hemisphere current vortex, which results in a weak eastward current over CGH in 1841–1842, compared to nearly no east-west directed current in 2010. Still, in general, the agreement between the observations and the model simulations is not that good, probably because CGH is located close to the *Sq* focus track, where variations in the *X* component are small and not very indicative of the large-scale features of the vortex.

At SIN we only have historical observations of magnetic perturbations, as there is no nearby modern-day station with data available. However, this station is located in a part of the world where the main magnetic field has changed relatively little (see Figure 2). Both model simulations show a similar daily variation in the *X* component as is seen in the historical observations, although the model gives a smaller peak that occurs later than observed. This was also the case for SHE, which in 1841–1842 was located at a similar distance from the magnetic equator. This indicates that the observations are reliable and that the differences with the model are systematic. There is little difference between the 1841–1842 and 2010 simulations, suggesting that the magnetic variations at SIN remained similar between 1841–1842 and 2010, although we cannot verify this with observations. For the whole period we consider here, the magnetic equator is located ~750 km or more to the north of SIN and therefore we do not expect magnetic data from this location to be affected by the equatorial electrojet.

### 4.2. *Y* Variations at GRW, SHE, CGH, and SIN: 1841–1842 Versus 2010

The magnetic variations in the *Y* component at GRW (Figure 3a) mostly show the characteristic pattern of an increase in the morning, associated with the southward branch of the *Sq* current vortex as it passes over the station, followed by a decrease in the afternoon, associated with the northward branch of the *Sq* current vortex. This pattern is strongest and clearest around June solstice, as would be expected because of the higher ionospheric conductivity during that season at GRW.

For June solstice the observed magnetic variations for 1841–1842 and 2010 match very closely, unlike the simulated variations, which show a phase shift between 1841–1842 and 2010. This phase shift is caused by a change in the shape of the *Sq* current vortex in the Northern Hemisphere, which results in the north-south

branches of the vortex to sweep past GRW earlier in the day in 2010 than in 1841–1842. This can be inferred from Figure 4. Over the course of a day, the foci of the *Sq* current vortices appear to migrate westward, as they stay roughly at the subsolar point (12 LT) while the Earth rotates underneath the *Sq* current system. At 12 UT, the Northern Hemisphere current focus is located farther west for the 2010 simulation than for the 1841–1842 simulation, and GRW already finds itself on the northward branch of the current vortex at this time, while in 1841–1842 GRW is located still on the westward branch of the current vortex. However, given that the observations do not show such a phase shift, this feature is clearly not realistic. For the equinoxes and December solstice the observations do indicate some differences between the daily variation of the *Y* component in 1841–1842 and 2010, but these are not correctly reproduced by the model. We can therefore not explain what might have caused these differences.

The *Y* magnetic variations at SHE (Figure 3b) consist mainly of a decrease in the morning and an increase in the afternoon, as expected for a station in the Southern Hemisphere. In addition, a small peak can be seen around 6–8 UT for the June solstice and equinox seasons. The observations show a larger afternoon peak in 2010 than in 1841–1842, which also occurs ~2 h later in the day around December solstice and the equinoxes. The model simulations also show an increase in this afternoon peak, although not exactly to the same degree, but do not reproduce the phase shift for December solstice and equinox. The observed morning decrease is also larger in 2010 than in 1841–1842 for June solstice and equinox, but this is not reproduced by the model either. The reduction in the peak around 6–8 UT that is observed for June solstice and equinox is only reproduced by the model for June solstice. As expected for a station close to the magnetic equator, east-west magnetic field variations are difficult to interpret. We therefore conclude that changes in the main magnetic field may be responsible for some but perhaps not all of the differences in the *Y* variations at SHE.

The daily variation in the *Y* component at CGH (Figure 3c) shows again mainly the characteristic trough in the morning followed by a peak in the afternoon. In general, the observed amplitude of this daily variation is larger in 2010 than in 1841–1842 and especially the amplitude of the afternoon peak. The model simulations also show a larger afternoon peak for 2010 but at the same time a weaker morning trough. The simulations can therefore only explain part of the observed differences between 1841–1842 and 2010.

The daily magnetic variations at SIN in the *Y* component (Figure 3d) are generally quite small, because the station is located close to the zero line between the Northern and Southern Hemisphere current vortices, where there is no strong north-south directed current. The model simulations indicate only small differences in the magnetic variations between 1841–1842 and 2010. We would therefore not expect to observe large differences between the magnetic variations in 1841–1842 and 2010 either, but unfortunately there were no stations operational in the vicinity of SIN in 2010 to verify this.

### 4.3. *D* Variations at ROM and MAN: 1782–1783 Versus 2010

Figures 5a and 5b show the daily variation in *D* for ROM and MAN. Measurements were only made three times per day in 1782–1783, so that the daily variation cannot be very clearly seen. However, the 1782–1783 observations are generally in reasonable agreement with modern-day measurements, including the significant seasonal changes in ROM, which suggests that they are of good quality. A hypothetical time error of 30 min as mentioned in section 2 would affect neither the general picture of the daily variation nor our analysis.

Observed differences between 1782–1783 and 2010 are generally larger for MAN than for ROM. In particular, the daytime trough at MAN is consistently deeper for 1782–1783 than for 2010 for all seasons, suggesting that the amplitude of the daily variation in *D* was somewhat larger in 1782–1783 than in 2010, although this is difficult to say for sure based on just three values to characterize the daily variation. Still, the model simulations also indicate a reduction in the amplitude of the daily magnetic variation at MAN from 1782–1783 to 2012 and are thus consistent with the observational result in this aspect. The model results indicate that the amplitude reduction is due to a change in the position and shape of the *Sq* current vortex which reduces the north-south component of the current passing over both ROM and MAN (not shown). However, the simulated daily variation at both MAN and ROM does in most cases not agree that well with the observed daily variation for 2010. We must therefore question also whether the simulated changes in the *Sq* current vortex between 1782–1783 and 2010 are realistic and cannot conclude firmly that the observed differences in the *D* variation at ROM and MAN are due to changes in the geomagnetic main field between these epochs.

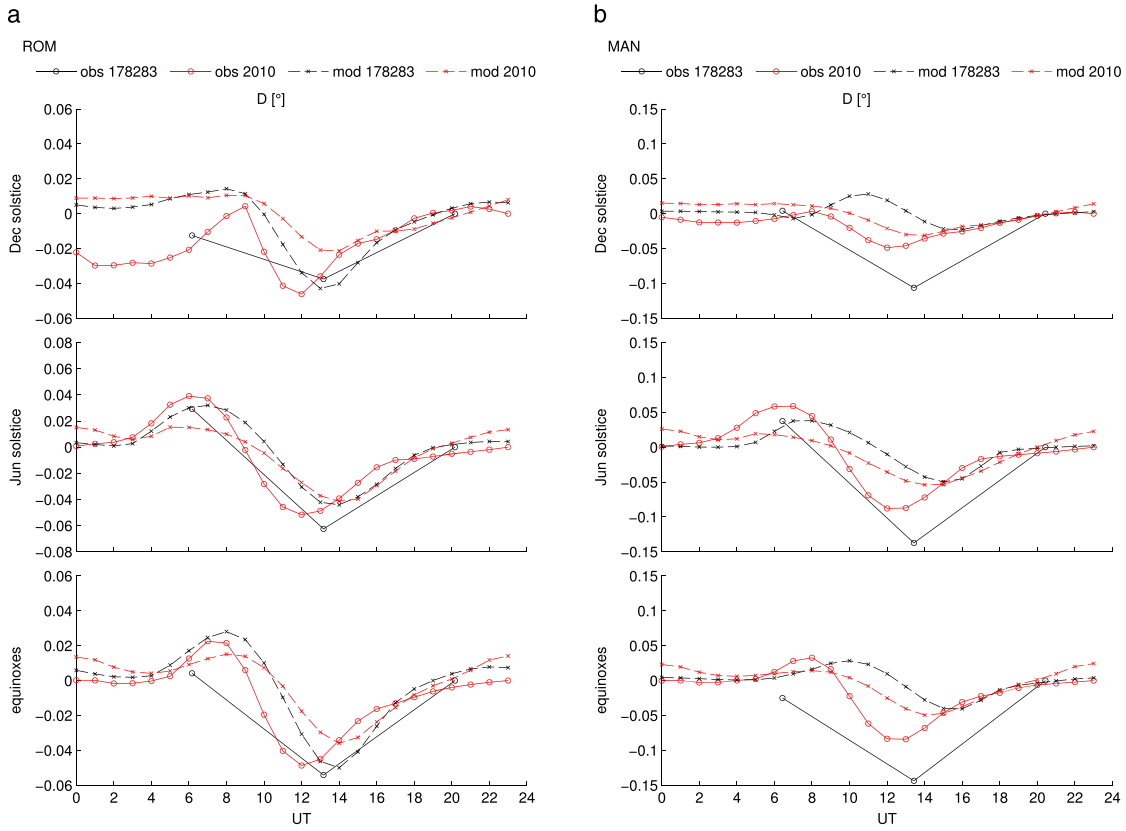


**Figure 5.** (a) Daily magnetic variations in the *D* component at ROM around (top) December solstice, (middle) June solstice, and (bottom) the equinoxes as observed (solid lines/open circles) and simulated (dashed lines/crosses) in 1782–1783 (black) and 2010 (red). (b) Same as Figure 5a but for MAN.

### 4.4. Differences in Magnetic Perturbations: 1652–1653 Versus 2010

So far we have concentrated on the effects of changes in the main magnetic field on the daily *Sq* variation, as our simulations indicated that this was a more important factor in causing differences between 2010 and the two historical periods we studied (1782–1783 and 1841–1842) than differences in solar activity. However, the solar activity level was similar for all these periods. In fact, we deliberately tried to match the solar activity for the different epochs we compared here to avoid effects associated with the ~11 year solar cycle as much as possible, because our study is concerned with long-term (multidecadal to multicentennial) changes in daily magnetic variations rather than those that occur on shorter timescales. On the timescale of a solar cycle, the effects of solar activity variations on the *Sq* system will certainly be much stronger than the effects of a change in the main field. Still, solar activity also varies on timescales longer than a solar cycle. The change in solar activity level from the Maunder Minimum period to the present day is a good example of this. Here we explore briefly how the effects of such a long-term change in solar activity compares with the effects of changes in the main magnetic field on the *Sq* current system.

An increase in solar activity level results primarily in an increase of the overall strength of the current vortices, without much effect on their location or shape (see supporting information). The increase in solar activity level from 60 to 95 sfu for the 1652–1653 simulations gives an increase in the magnitude of the equivalent *Sq* current foci of a factor ~1.3 on average (it is slightly larger in the winter hemisphere and slightly smaller in the summer hemisphere). This is in good agreement with results obtained by *Yamazaki and Kosch* [2014], who found a square root relationship between $F_{10.7}$ and *Sq*, implying that a change in $F_{10.7}$ from 60 to 80, 85, and 95 sfu increases the *Sq* signal by a factor of 1.15, 1.19, and 1.25, respectively.

A factor of 1.3 difference in the magnitude of the *Sq* signal can be of a comparable order of magnitude to the effects of a change in the main magnetic field, but this obviously depends on the epochs that are being compared and on the location. This is illustrated in Figure 6, which shows the daily magnetic variation for equinox

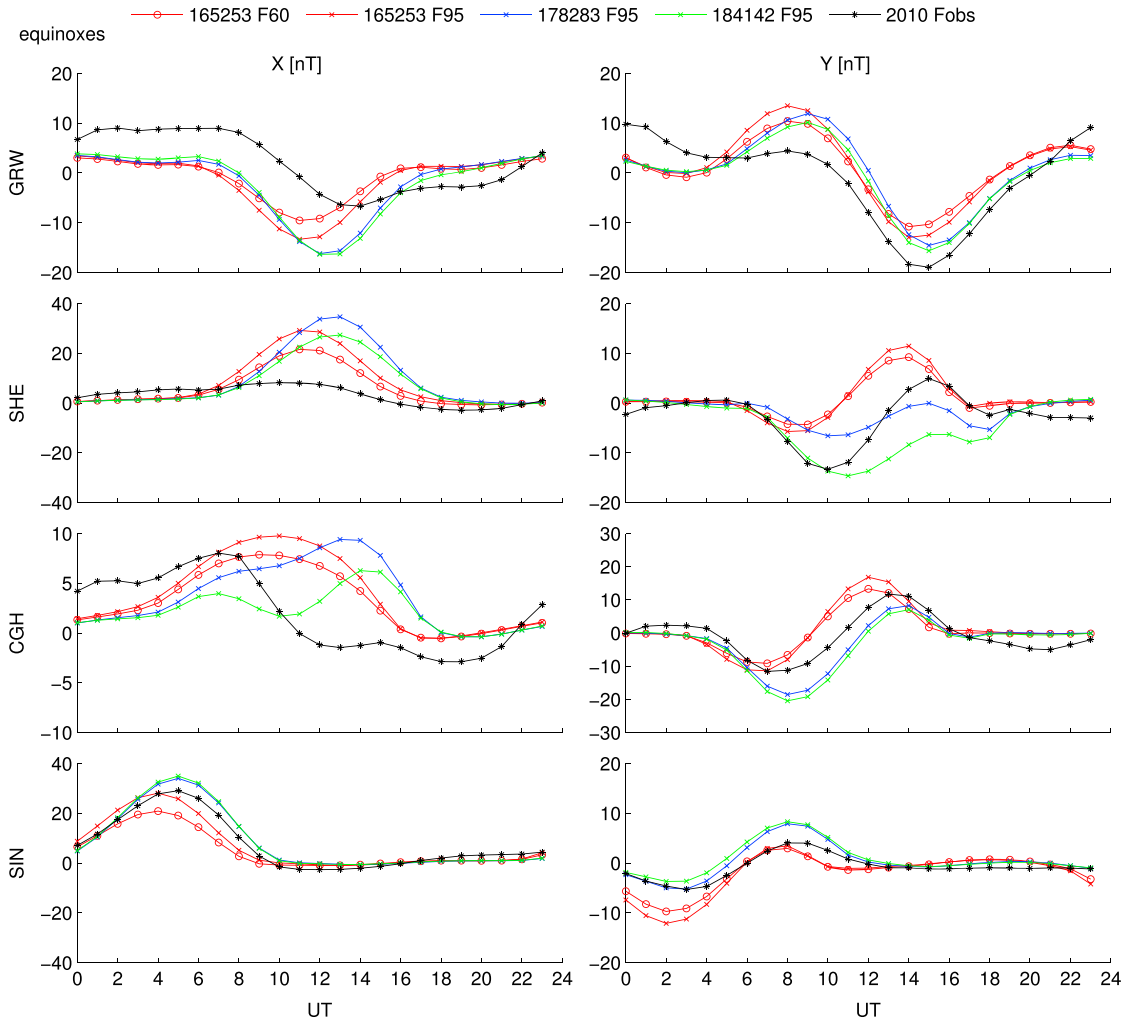


**Figure 6.** Simulated daily magnetic variations for the equinox season in the (left column) *X* and (right column) *Y* components at GRW, SHE, CGH, and SIN (from top to bottom) for 1652–1653 (red), 1782–1783 (blue), 1841–1842 (green), and 2010 (black). Simulations with $F_{10.7}$ set to 95 sfu are marked with crosses, while open circles mark $F_{10.7}$ set to 60 sfu (1652–1653), and stars mark observed $F_{10.7}$ values (2010).

conditions at four of the stations we studied before (GRW, SHE, CGH, and SIN) for five different simulations. Three of these simulations were run with the same, fixed solar activity level of 95 sfu but different main magnetic fields (those of 1652–1653, 1782–1783, and 1841–1842), while the two other simulations were run with the main magnetic field of 1652–1653 but a lower solar activity level (60 sfu) and with the main magnetic field of 2010 and variable solar activity level according to observations (on average ~80 sfu), respectively.

Effects of changes in the Earth's magnetic field are small in some cases, e.g., when comparing 1782–1783 and 1841–1842 at GRW and SIN, but large in other cases, e.g., when comparing the *Y* component at SHE or the *X* component at CGH for those same epochs. GRW, SHE, and CGH all show a relatively large difference between the 2010 simulation and any of the simulations for historical epochs, while those differences are much smaller for SIN. This is because GRW, SHE, and CGH are all located within a longitude sector that has experienced relatively large main magnetic field changes between 2010 and the historical epochs, while SIN is located in a region where main magnetic field changes have been much smaller throughout the last 400 years. At such locations long-term changes in solar activity on the order of 35 sfu are of similar importance to main magnetic field changes in causing long-term changes in the daily magnetic variation. However, in regions more strongly affected by the expansion and northwestward movement of the South Atlantic Anomaly of the main magnetic field, roughly 100°W–30°E, changes in the main magnetic field are more important in causing long-term changes in the daily magnetic variation on the ground.

## 5. Summary and Conclusions

We compared historical magnetic measurements from the eighteenth and nineteenth centuries with modern-day data for several geomagnetic observatories. The daily magnetic variations in 1782–1783 at ROM and MAN and in 1841–1842 at GRW, SHE, CGH, and SIN revealed notable differences with daily magnetic variations observed at nearby stations (where available) in 2010. Further comparisons with model simulations showed that differences in solar activity level between these epochs were too small to explain the differences between the historical and modern-day observations. However, changes in the main magnetic field could explain at least some of the observed differences.

Changes in the main magnetic field affect the daily magnetic variation observed on the ground in two main ways. First, changes in the structure of the magnetic field, particularly movements of the magnetic equator, affect the shape and positioning of the two equivalent current vortices in the ionosphere that are responsible for the magnetic perturbations on the ground. A ground-based station may therefore rotate underneath a different part of the current system as the main field changes and therefore experience different magnetic variations. Second, changes in the main magnetic field intensity affect the conductivity of the ionosphere, which can also affect the shape of the current vortices, as well as their overall strength.

Not all the observed differences between the historical and modern-day magnetic variations could be explained by the effects of changes in the Earth's main magnetic field as simulated by the model. This is likely to be partly due to model deficiencies. As expected due to the TIE-GCM generally underestimating *E* region conductivities, the amplitude of the observed magnetic perturbations were often larger than predicted by the model. Also, observations and model simulations were usually in better agreement for the magnetic component that characterizes the large-scale features of the *Sq* current system, while discrepancies were larger in the other component, i.e., the *X* component for stations close to the *Sq* focus track and the *Y* component for stations close to the dip equator. There may also be other factors that contributed to the differences between the simulated and observed magnetic perturbations, relating to other drivers of long-term change in the observations that were not included in the simulations, such as long-term changes in upwardly propagating tides under the influence of climate change in the lower atmosphere. This possibility should be investigated in future research.

In addition, when the difference in solar activity is larger than the differences between the epochs we studied here with observational data, this could also become an important factor. Our model simulations showed that a difference in solar activity level of 35 sfu, as indicated by the $F_{10.7}$ index, changes the strength of the ionospheric currents by a factor ~1.3. This difference in solar activity indicates the difference between fairly normal solar minimum conditions ($F_{10.7} = 95$ sfu) and unusually low solar activity conditions as occurred during the Maunder Minimum ($F_{10.7} = 60$ sfu). It is therefore indicative of a long-term (multicentennial) change in solar activity. In regions where main magnetic field changes over the past few centuries have been relatively small, such as at SIN, the effects of such a long-term change in solar activity are comparable in magnitude to the effects of multicentennial changes in the main field. However, in regions where the main magnetic field has undergone relatively large changes, such as in the vicinity of the South Atlantic Anomaly region, these main field changes are generally more important in causing long-term changes in the daily magnetic variations on the ground than long-term changes in solar activity.

**Acknowledgments**

The modern observations for 2010 presented in this paper rely on data collected at various magnetic observatories. We thank the Istituto Nazionale di Geofisica e Vulcanologia (INGV), Rome, for data from AQU; the University Stuttgart and the Karlsruhe Institute of Technology (KIT), for data from BFO; BGS, Edinburgh, for data from HAD; the South African National Space Agency (SANSA), Hermanus, for data from HER; GFZ, Potsdam, for data from SHE; and INTERMAGNET for promoting high standards of magnetic observatory practice (www.intermagnet.org). We further thank BGS for operating the WDC for Geomagnetism, Edinburgh, and for providing digital copies of historical geomagnetic observatory yearbooks (http://www.geomag.bgs.ac.uk/data_service/data/yearbooks/yearbooks.html). We are grateful to Natasha Krivova for providing us with the $F_{10.7}$ reconstruction going back to 1610 and to Claudia Stolle for helpful discussions. The $F_{10.7}$ reconstruction can be obtained directly from N. Krivova on request (e-mail: krivova@mps.mpg.de). The TIE-GCM simulations analyzed here were performed on the ARCHER UK National Supercomputing Service (http://www.archer.ac.uk), funded through NERC fellowship grant NE/J018058/1. Model output will be made freely available to the scientific community on request (contact I. Cnossen; icnossen@yahoo.com).

## References

Airy, G. B. (1843), *Magnetical and Meteorological Observations Made at the Royal Observatory, Greenwich, in the Years 1840 and 1841*, Board of Admiralty, London.

Airy, G. B. (1846), *Magnetical and Meteorological Observations Made at the Royal Observatory, Greenwich, in the Year 1842*, Board of Admiralty, London.

Briggs, B. H. (1984), The variability of ionospheric dynamo currents, *J. Atmos. Terr. Phys.*, *46*, 419–429, doi:10.1016/0021-9169(84)90086-2.

Camuffo, D. (2002), Errors in early temperature series arising from changes in style of measuring time, sampling schedule and number of observations, *Clim. Change*, *53*, 331–352.

Cnossen, I. (2014), The importance of geomagnetic field changes versus rising $CO_2$ levels for long-term change in the upper atmosphere, *J. Space Weather Space Clim.*, *4*, A18, doi:10.1051/swsc/2014016.

Cnossen, I., and A. D. Richmond (2008), Modelling the effects of changes in the Earth's magnetic field from 1957 to 1997 on the ionospheric $h_mF_2$ and $f_oF_2$ parameters, *J. Atmos. Sol. Terr. Phys.*, *70*, 1512–1524, doi:10.1016/j.jastp.2008.05.003.

Cnossen, I., and A. D. Richmond (2012), How changes in the tilt angle of the geomagnetic dipole affect the coupled magnetosphere-ionosphere-thermosphere system, *J. Geophys. Res.*, *117*, A10317, doi:10.1029/2012JA018056.

Cnossen, I., and A. D. Richmond (2013), Changes in the Earth's magnetic field over the past century: Effects on the ionosphere-thermosphere system and solar quiet (*Sq*) magnetic variation, *J. Geophys. Res. Space Physics*, *118*, 849–858, doi:10.1029/2012JA018447.

Cnossen, I., A. D. Richmond, M. Wiltberger, W. Wang, and P. Schmitt (2011), The response of the coupled magnetosphere-ionosphere-thermosphere system to a 25% reduction in the dipole moment of the Earth's magnetic field, *J. Geophys. Res.*, *116*, A12304, doi:10.1029/2011JA017063.

Cnossen, I., A. D. Richmond, and M. Wiltberger (2012), The dependence of the coupled magnetosphere-ionosphere-thermosphere system on the Earth's magnetic dipole moment, *J. Geophys. Res.*, *117*, A05302, doi:10.1029/2012JA017555.

De Haro Barbas, B. F., A. G. Elias, I. Cnossen, and M. Zossi de Artigas (2013), Long-term changes in solar quiet (*Sq*) geomagnetic variations related to Earth's magnetic field secular variation, *J. Geophys. Res. Space Physics*, *118*, 3712–3718, doi:10.1002/jgra.50352.

Doumbia, V., A. Maute, and A. D. Richmond (2007), Simulation of equatorial electrojet magnetic effects with the thermosphere-ionosphere-electrodynamics general circulation model, *J. Geophys. Res.*, *112*, A09309, doi:10.1029/2007JA012308.

Elias, A. G., M. Zossi de Artigas, and B. F. De Haro Barbas (2010), Trends in the solar quiet geomagnetic field variation linked to the Earth's magnetic field secular variation and increasing concentrations of greenhouse gases, *J. Geophys. Res.*, *115*, A08316, doi:10.1029/2009JA015136.

Elliot, C. M. (1851), *Magnetical Observations Made at the Honourable East India Company's Magnetical Observatory at Singapore*, The American Mission and Male Asylum Presses, Madras.

Hansteen, C. (1819), *Untersuchungen über den Magnetismus der Erde*, Lehmann and Gröndahl, Christiania.

Hemmer, J. J. (1783), *Ephemerides Societatis Meteorologicae Palatinae, Historia et Observationes 1781*, Schwan, Mannheim.

Hemmer, J. J. (1784), *Ephemerides Societatis Meteorologicae Palatinae Observationes Anni 1782*, Schwan, Mannheim.

Hemmer, J. J. (1785), *Ephemerides Societatis Meteorologicae Palatinae Observationes Anni 1783*, Schwan, Mannheim.

Jackson, A., A. R. T. Jonkers, and M. R. Walker (2000), Four centuries of geomagnetic secular variation from historical records, *Phil. Trans. R. Soc. Lond. A*, *358*, 957–990, doi:10.1098/rsta.2000.0569.

Korte, M., M. Mandea, and J. Matzka (2009), A historical declination curve for Munich from different data sources, *Phys. Earth Planet. Inter.*, *177*, 161–172, doi:10.1016/j.pepi.2009.08.005.

Krivova, N. A., L. E. A. Vieira, and S. K. Solanki (2010), Reconstruction of solar spectral irradiance since the Maunder minimum, *J. Geophys. Res.*, *115*, A12112, doi:10.1029/2010JA015431.

Kuvshinov, A. (2008), 3-D global induction in the ocean and solid Earth, Recent progress in modeling magnetic and electric fields from sources of magnetospheric, ionsopheric and oceanic origin, *Surv. Geophys.*, *29*, 139–186, doi:10.1007/s10712-008-9045-z.

Kuvshinov, A., C. Manoj, N. Olsen, and T. Sabaka (2007), On induction effects of geomagnetic daily variations from equatorial electrojet and solar quiet sources at low and middle latitudes, *J. Geophys. Res.*, *112*, B10102, doi:10.1029/2007JB004955.

Macmillan, S., and A. Droujinina (2007), Long-term trends in geomagnetic daily variation, *Earth Planets Space*, *59*, 391–395, doi:10.1186/BF03352699.

Matzka, J. (2016), Geomagnetic Observatory St. Helena, preliminary hourly mean values 2010, XYZ components, GFZ Data Services. [Available at http://doi.org/10.5880/GFZ.2.3.2016.001.]

Matzka, J., A. Chulliat, M. Mandea, C. C. Finlay, and E. Qamili (2010), Geomagnetic observations for main field studies: From ground to space, *Space Sci. Rev.*, *155*, 29–64.

Murison, M., A. D. Richmond, and S. Matsushita (1985), Estimation of ionospheric electric fields and currents from a regional magnetometer array, *J. Geophys. Res.*, *90*, 3525–3530, doi:10.1029/JA090iA04p03525.

Rastogi, R. G., and K. N. Iyer (1976), Quiet day variation of geomagnetic *H*-field at low latitudes, *J. Geomag. Geoelectr.*, *28*, 461–479, doi:10.5636/jgg.28.461.

Richmond, A. D. (1995), Ionospheric electrodynamics, in *Handbook of Ionospheric Electrodynamics*, vol. 2, pp. 249–290, CRC Press, Boca Raton, Fla.

Richmond, A. D., and A. Maute (2014), Ionospheric electrodynamics modelling, in *Modeling the Ionosphere/Thermosphere System*, edited by J. Huba, R. Schunk, and G. Khazanov, *Am. Geophys. Union Monogr. Ser.*, 201, pp. 57–73, John Wiley, Chichester, U. K., doi:10.1002/9781118704417.ch6.

Richmond, A. D., E. C. Ridley, and R. G. Roble (1992), A thermosphere/ionosphere general circulation model with coupled electrodynamics, *Geophys. Res. Lett.*, *19*, 601–604, doi:10.1029/92GL00401.

Rishbeth, H., and R. G. Roble (1992), Cooling of the upper atmosphere by enhanced greenhouse gases – Modelling of thermospheric and ionospheric effects, *Planet. Space Sci.*, *40*, 1011–1026, doi:10.1016/0032-0633(92)90141-A.

Roble, R. G., E. C. Ridley, and A. D. Richmond (1988), A coupled thermosphere/ionosphere general circulation model, *Geophys. Res. Lett.*, *15*, 1325–1328, doi:10.1029/GL015i012p01325.

Sabine, E. (1847), *Observations Made at the Magnetical and Meteorological Observatory at St. Helena*, vol. I 1840, 1841, 1842 and 1843, Her Majesties Stationary Office, London.

Sabine, E. (1851), *Observations Made at the Magnetical and Meteorological Observatory at the Cape of Good Hope*, vol. I Magnetical observations 1841 to 1846, Her Majesties Stationary Office, London.

Schlapp, D. M., R. Sellek, and E. C. Butcher (1990), Studies of worldwide secular trends in the solar daily geomagnetic variation, *Geophys. J. Int.*, *100*, 469–475, doi:10.1111/j.1365-246X.1990.tb00699.x.

Sellek, R. (1980), Secular trends in daily geomagnetic variations, *J. Atmos. Terr. Phys.*, *42*, 689–695, doi:10.1016/0021-9169(80)90052-5.

Shinbori, A., Y. Koyama, M. Nose, T. Hori, Y. Otsuka, and A. Yatagai (2014), Long-term variation in the upper atmosphere as seen in the geomagnetic solar quiet daily variation, *Earth Planets Space*, *66*, 155, doi:10.1186/s40623-014-0155-1.

Takeda, M. (2013), Contribution of wind, conductivity, and geomagnetic main field to the variation in the geomagnetic *Sq* field, *J. Geophys. Res. Space Physics*, *118*, 4516–4522, doi:10.1002/jgra.50386.

Thébault, E., et al. (2015), International Geomagnetic Reference Field: The 12th generation, *Earth Planets Space*, *67*, 79, doi:10.1186/s40623-015-0228-9.

Torta, J. M, L. R. Gaya-Piqué, J. J. Curto, and D. Altadill (2009), An inspection of the long-term behaviour of the range of the daily geomagnetic field variation from comprehensive modelling, *J. Atmos. Sol. Terr. Phys.*, *71*, 1497–1510.

Winkler, P. (2009), Revision and necessary correction of the long-term temperature series of Hohenpeissenberg, 1781–2006, *Theor. Appl. Climatol.*, *98*, 259–268, doi:10.1007/s00704-009-0108-y.

Yamazaki, Y., and M. J. Kosch (2014), Geomagnetic lunar and solar daily variations during the last 100 years, *J. Geophys. Res. Space Physics*, *119*, 6732–6744, doi:10.1002/2014JA020203.

Yamazaki, Y., K. Yumoto, T. Uozumi, S. Abe, M. G. Cardinal, D. McNamara, R. Marshall, B. M. Shevtsov, and S. I. Solovyev (2010), Reexamination of the *Sq*-EEJ relationship based on extended magnetometer networks in the East Asian region, *J. Geophys. Res.*, *115*, A09319, doi:10.1029/2010JA015339.

Yamazaki, Y., et al. (2011), An empirical model of the quiet daily geomagnetic field variation, *J. Geophys. Res.*, *116*, A10312, doi:10.1029/2011JA016487.